

# PREPARATION OF GOLD NANOPARTICLES STABILIZED BY CHITOSAN USING IRRADIATION AND SONICATION METHODS

**Renata Czechowska-Biskup\*, Bożena Rokita, Piotr Ulański,  
Janusz M. Rosiak**

*Institute of Applied Radiation Chemistry, Faculty of Chemistry  
Lodz University of Technology,  
ul. Wroblewskiego 15, 93-590 Lodz, Poland.  
e-mail: czechow@mitr.p.lodz.pl*

## **Abstract**

*Gold nanoparticles (AuNPs) were synthesized, in the absence of any reducing agent, using ionizing radiation or ultrasound in aqueous solutions of chloroauric acid (HAuCl<sub>4</sub>). Chitosan (average molecular weight 158 kDa, degree of deacetylation 90 %) was used as a stabilizing agent. Both techniques yielded AuNPs which were stable in solution at RT for at least 3 months after synthesis. UV-Vis spectroscopy was used to follow substrate decay, nanoparticles formation, size of the gold core and particles stability. Hydrodynamic radii and polydispersion of the chitosan-stabilized AuNPs (i.e. the whole core-shell nanoparticles) were determined by dynamic light scattering. Zeta potential measurements were performed to assess the surface charge and stability of the particles. Influence of synthesis parameters and presence of isopropanol on the formation and properties of the products have been described and reaction mechanisms have been discussed. Radiation and sonochemical methods are demonstrated to be very efficient, fast and easy-to-control methods of synthesizing gold nanoparticles, leaving behind no unreacted reducing agent or unwanted side products, while stabilization by chitosan provides AuNPs with excellent stability and long shelf life.*

**Keywords:** *gold nanoparticles, chitosan, stabilization, irradiation, sonication*

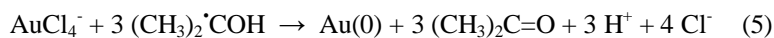
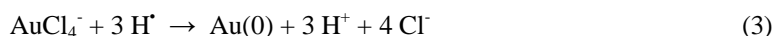
**Received:** 18.02.2015

**Accepted:** 14.05.2015

## 1. Introduction

Gold nanoparticles (AuNPs) due to their unique optical, electrical and catalytic properties are used in many areas of life, mainly in medicine, electronics and technologies of manufacturing modern materials [1,2]. Their small size, high surface area-to-volume ratio and stability at high temperatures make them perfect tool in medical diagnostics, photodynamic therapy as well as in the active transport of drugs, especially for cancer treatment [3]. Gold nanoparticles are employed in radiotherapy, in two modes – to increase local dose deposition in tissue during radiotherapy or as a local emitter of gamma and beta rays. In the latter case, the nanoparticles contain radioactive gold isotopes ( $^{198}\text{Au}$ ) [4,5]. Gold-198 ( $\gamma$  412 keV,  $\beta^-$  0,96 MeV) has range in tissue of about 0.38 mm and half-life 2.7 days, it can be used to imaging and localization in biodistribution studies [6].

Up to now, a number of methods have been used to prepare AuNPs, mainly involving reduction of gold salt in aqueous solution by various reducing chemical agents such as sodium borohydride or sodium citrate [7]. However in these methods unreacted substrates and byproducts are difficult to remove after synthesis and can influence the purity of particles. Physicochemical methods such as radiation- and sonochemical synthesis of gold nanoparticles (of partially similar mechanisms of reduction of gold) can be classified as environmentally friendly techniques, since no chemical reducing agents are used and no side products are formed. In radiation synthesis metal nanoparticles are obtained by reduction of metal ions to atoms in reactions with radiolytically generated hydrated electrons ( $e_{\text{aq}}^-$ ) and hydrogen atoms (H) resulting from radiolysis of water [8-10], while in sonochemistry, where no hydrated electrons are formed, the reducing agents are hydrogen atoms and, optionally, also hydroxyalkyl radicals if alcohols are used as co-solvent [11]. Basic reactions involved in the radiation synthesis of AuNPs, taking chloroaurate as the substrate, can be schematically described by eqns (1-3), with a potential participation of reactions (4-5), while the sonochemical synthesis is based on reaction (6), followed by (3-5).





In the last step, gold atoms coalesce to form clusters and finally nanoparticles:



The general scheme presented above is obviously a simplification. Processes depicted as (2), (3) and (5) are in fact multi-step reactions, further complicated by disproportionation reactions between gold species of various oxidation states. Furthermore, it has been shown that the final nanoparticles are composed not solely of gold atoms, but typically also incorporate some gold ions [12].

Due to high surface energy of gold nanoparticles and their tendency to aggregate during the synthesis and subsequent storage, there is a need to moderate the coalescence process and prevent aggregation. This is usually accomplished by addition of a suitable stabilizing agent. Polymers are used as compounds which can attach to and form a layer around the individual nanoparticles, causing their stabilization. Actually, a complex nanoparticle is formed in this way, with a metal core and polymer shell. Often, albeit not always, the chosen polymer is a polyelectrolyte, which renders the particles high surface charge. Coulombic repulsive forces between the particles bearing high charge of the same sign prevents them from aggregation. One of the polyelectrolytes being studied with this respect is chitosan, polysaccharide of natural origin, classified as a stabilizer which improves the dispersion stability due to the presence of the protonated amino groups. Chitosan is generally recognized as being non-toxic, biocompatible and biodegradable, and it has many other interesting properties, especially valuable for the prospective biomedical applications [13-15]. Previous studies on stabilization of AuNP by chitosan indicated that chitosan can act not only as a stabilizer, but also as a reducing agents of gold salt [16]. Using chitosans of different molecular weight as a stabilizer, one can obtain AuNP with different size distributions [17].

So far, there are few works where the influence of chitosan on the stabilization of gold nanoparticles synthesized by irradiation or sonochemical technique was examined. Vo et al. reported the influence of type of irradiation (e-beam vs. gamma rays) and pH on formation of gold nanoparticles stabilized by low molecular weight chitosan [18, 19]. They tried to explain the mechanism of interaction between  $\text{AuCl}_4^-$  and glucosamine moieties of chitosan molecules. They found that complexation between Au(III) and monomer units of chitosan occurs only above pH 3.5 and has some influence on size of obtained AuNPs. To our best knowledge, only one work is related to the sonochemical formulation of gold nanoparticles in the presence of chitosan [20]. Okitsu et al. sonicated aqueous solution of  $\text{Na}[\text{AuCl}_4]$  in a system containing chitosan powder. After reduction of Au(III), gold nuclei and then larger clusters were formed.

Obtained nanoparticles adsorbed onto the surface of chitosan particles, thus in a sense chitosan powder acted in this system as a kind of stabilizer.

The use of irradiation to produce gold nanoparticles is a promising method, but the availability of sources of ionizing radiation is limited. We believe that the use of ultrasound to synthesis of gold nanoparticles may be an interesting alternative, allowing, as the radiation method, to skip the chemical reducing agents, but being more readily available than irradiation. In this paper we describe synthesis of gold nanoparticles stabilized by chitosan using ionizing radiation (electron beam) and ultrasound, and we compare the products resulting from these two methods. We also demonstrate how the reaction conditions influence the efficiency of AuNP formation and their properties.

## **2. Materials and Methods**

### **2.1. Chemicals/Materials**

Medical grade chitosan was obtained from Heppe Medical Chitosan GmbH (Germany). Viscosity-average molecular weight of this chitosan was 158 kDa (our own measurement in 0.2 mol dm<sup>-3</sup> acetic acid / 0.15 mol dm<sup>-3</sup> ammonium acetate at 25.0 °C [21]) while the deacetylation degree was 88 % as stated by the manufacturer. HAuCl<sub>4</sub> of high purity grade was purchased from Alfa Aesar. All other chemicals were of p.a. or equivalent quality. High-purity water (0.055 μS cm<sup>-1</sup>, TKA MicroPure system) was used in all experiments.

Chitosan ( $2 \times 10^{-3}$  mol dm<sup>-3</sup> (in terms of monomer units bearing amine groups, equivalent to 0.322 g dm<sup>-3</sup>) was dissolved completely in 100 ml of  $5 \times 10^{-2}$  mol dm<sup>-3</sup> acetic acid for 24 h. Next day chloroauric acid was added ( $1 \times 10^{-3}$  mol dm<sup>-3</sup>) optionally followed by addition of isopropanol (0.2 mol dm<sup>-3</sup>). Aqueous solutions were made up in ultrapure water. Solution was poured into flat-bottom glass ampoules of 10 ml capacity.

### **2.2. Irradiation by electron beam**

Before irradiation samples were degassed by argon saturation. Solutions in ampoules were irradiated at room temperature with 1 kGy, 2 kGy, 5 kGy and 10 kGy doses of 6 MeV electrons from a linear electron accelerator (ELU-6e, Russia). Irradiation was carried out using a pulsed electron beam (pulse frequency 20 Hz, pulse duration 4 μs). Average dose rate was 95 Gy s<sup>-1</sup>, as determined by alanine dosimetry (e-scan, Bruker) [22].

### **2.3. Sonication**

Sonications were performed in a URS-1000 ultrasonic reactor setup (Allied Signal Elac-Nautik, Kiel, Germany), consisting of a CESAR wave generator and amplifier, ultrasonic transducer and a thermostated cylindrical reactor of 500 ml capacity. The vibrating element of the transducer, covered with stainless steel, formed the bottom of the reactor. The reactor was filled with water, and the sample (10 ml) was contained in a gas-tight, flat-bottom glass ampoule placed at a fixed position in the central part of the reactor (the water level in

the reactor was higher than the level of the solution in the ampoule). Before sonication the samples were saturated with argon for 20 minutes in order to remove oxygen. Ultrasound power, dose rate and frequency were 50 W, 74 W kg<sup>-1</sup> (equivalent to Gy s<sup>-1</sup>) and 620.2 kHz, respectively. Sonication was performed at 20 °C for 5, 20 and 30 minutes.

## 2.4. Characterization of gold nanoparticles

### 2.4.1. UV-Vis Spectroscopy

The UV-Vis spectra of the gold dispersion were recorded at a resolution of 2 nm in the range of 190-800 nm using a Lambda40 spectrophotometer (Perkin Elmer Instruments), in quartz cells with an optical path of 1 mm. Water was used as reference.

### 2.4.2 DLS and $\zeta$ potentials measurements

Hydrodynamic diameter and  $\zeta$  (zeta) potential of gold nanoparticles were measured using ZetaSizer Nano ZS (Malvern Instruments Ltd.) equipped with a 633 nm laser.

Nanoparticle size was calculated on the basis of cumulative analysis. The particle size is defined as a Z-average diameter (Z-Average). On the basis of the autocorrelation curve, polydispersity index (PDI) values were obtained, which indicate the width of the particle size distributions. This parameter is low, in the order of 0.10, for particles with a narrow size distribution and reach 1.00 for systems with very broad distributions.

$\zeta$  potential, being a measure of the surface charge of a (nano)particle, is one of the main factors affecting the interaction between the particles in liquid. If the value of this potential is more than 30 mV or less than -30 mV, the repulsive forces between particles are large enough to stabilize the dispersion (solution). Lower (in absolute terms) values of  $\zeta$  potential lead to instability of dispersion, indicating a tendency to aggregation and / or precipitation.

## 3. Results and Discussion

### 3.1. Synthesis of gold nanoparticles and their characterization using UV-Vis spectroscopy

Formation and stability of gold nanoparticles can be conveniently followed by UV-visible spectroscopy. In general, AuNPs absorb light between 500 and 600 nm, depending on the particle size. As the size of nanoparticle increases, the plasmon absorption band shifts towards longer wavelengths [23].

When deoxygenated aqueous solutions containing  $1 \times 10^{-3}$  mol dm<sup>-3</sup> HAuCl<sub>4</sub>,  $2 \times 10^{-3}$  mol dm<sup>-3</sup> chitosan and 0.05 mol dm<sup>-3</sup> acetic acid (212 nm to keep the solutions acidic which is needed for chitosan solubilization) is subjected to ionizing radiation, the light yellow color of the initial solutions turns red or pink. Fig. 1a shows absorption spectra of the unirradiated solution, as well as solutions irradiated by various doses of high-energy electrons, while Fig. 1b shows corresponding samples to which 0.2 mol dm<sup>-3</sup> of isopropanol has been added before irradiation. The initial spectrum (before

irradiation) is dominated by a strong absorbance band in UV with a maximum at 212 nm. This band is mainly due to the presence of chloroaurate ions, with some contributions of chitosan and acetic acid. A shoulder at ca. 280-300 nm may be due to the presence of carbonyl groups in chitosan (mainly in acetylamino groups). Irradiation leads to significant changes in the spectrum. The band at 212 nm gradually disappears – it is totally absent for doses of 5 kGy and higher. In the low-wavelength end of the spectrum we can see the residual absorbance of acetic acid and chitosan; the band at ca. 280 nm seems to become more apparent, which may be due to formation of carbonyl groups in chitosan, a well-known side effect in radiolysis of this compound [24]. The decay of the 212 nm band is accompanied by a formation of a new, relatively broad band in the visible range, initially centered at ca. 530 nm. This band increases with dose and its maximum seems to undergo a blue shift, finally stabilizing at 518 nm at the highest doses used (510 nm for samples containing isopropanol). It should be noted that the increase in absorbance of the visible band was not proportional to dose in the whole tested range; rather it slowed down with dose indicating a tendency to reach a plateau. While the presence of isopropanol had some influence the evolution of the visible band with dose and the final location of the maximum, it apparently did not strongly influence on the final absorbance value.

Disappearance of the 212 nm band is due to the reduction of chloroaurate by solvated electrons and hydrogen atoms resulting from radiolysis of water. Formation of the broad band in the visible indicates the presence of gold nanoparticles. The maximum of absorption between 510-540 nm is characteristic for the surface plasmon resonance band of gold nanoparticles (AuNPs). Li et al. reported that absorbance in 522-550 nm range corresponds to AuNPs with sizes from 7 to 45 nm [25]. The observed dose influence and the actual location of the maxima observed in the final spectra shown in Fig. 1a (510-518 nm) indicates that average size of our AuNPs slightly decreases during the synthesis to reach finally the size in the order of ca. 5 - 10 nm.

Influence of isopropanol on the nanoparticles size (as evidenced by a shift in the band location) has been observed before [9]. It has been postulated that the alcohol molecules can adsorb on the surface of the gold nanoparticles and the adsorbed molecules of isopropanol stabilize the particles at a small size. However, the main rationale behind running the tests in the absence and presence of isopropanol was to see if any influence on the AuNP yield is observed. Out of three main products of water radiolysis (eqn. (1)),  $\cdot\text{OH}$  radicals are of strongly oxidising properties. While it is not clear if they can reverse the reduction of chloroaurate caused by hydrated electrons and H atoms, in the radiation synthesis procedure it seems reasonable to scavenge hydroxyl radicals using an alcohol, since the resulting hydroxyalkyl radicals have reducing properties and thus are expected to form additional AuNPs besides those formed by  $e_{\text{aq}}^-$  and H. In the systems tested here, however, this effect seems to be weak.

This may be in part due to the fact that both acetic acid and chitosan are fairly good scavengers of  $\cdot\text{OH}$  themselves, thus limiting the influence of isopropanol.

Chitosan seems to be a good stabilizer of AuNP at the first stages of the synthesis. No aggregation or precipitation during or immediately after the synthesis has been observed. Long-term stability is discussed in Chapter 3.3 below.

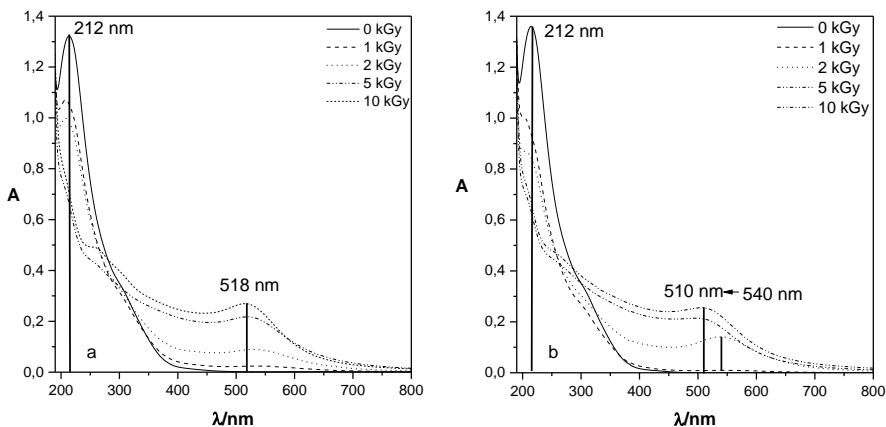


**Figure 1.** Absorption spectra of colloidal gold nanoparticles formed by irradiation of  $1 \times 10^{-3} \text{ mol dm}^{-3} \text{ H AuCl}_4$  in the presence of  $2 \times 10^{-3} \text{ mol dm}^{-3}$  chitosan in aqueous  $0.05 \text{ mol dm}^{-3}$  acetic acid solution at pH 2.8, a) without isopropanol, b) with  $0.2 \text{ mol dm}^{-3}$  isopropanol. Spectra recorded 20 minutes after irradiation.

Similar results have been obtained by Vo and co-workers [19]. In their work (no alcohol present) the intensity of the plasmon resonance band increased with doses and maximum absorption was around 520 nm.

Formation of AuNPs can be also achieved by the action of ultrasound (see Introduction). Our sonochemical tests were performed in order to identify conditions allowing for efficient AuNPs formation as well as to check if chitosan is a good stabilizing agent for sonochemically synthesized gold nanoparticles. Composition of solutions was identical as in the case of radiation experiments. Sonication, at the conditions applied, did not result in apparent AuNPs formation in the absence of isopropanol, while in the presence of isopropanol the spectral changes (Fig. 2) indicated successful nanoparticle synthesis – the absorbance at 212 nm was reduced, while a new band in the visible region was formed, similar, but not identical, to that observed as a result of irradiation. The broad band is initially located at ca. 533 nm, and during further sonication it shifts to ca. 556 nm, while its intensity increases almost linearly with sonication time (Fig. 3). Two facts, incomplete reduction of the substrate band

at 212 nm and absorbance values of the product band lower than observed in radiation experiments, indicate that even at the longest sonication time the transformation of the substrate into AuNPs must still have been incomplete.

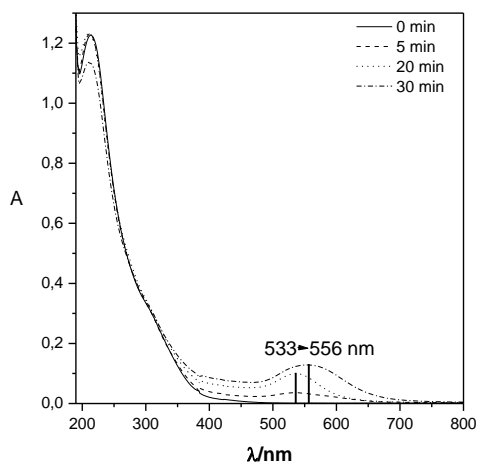


**Figure 2.** Absorption spectra of colloidal gold nanoparticles synthesized by sonication in  $2 \times 10^{-3}$  mol dm $^{-3}$  chitosan in aqueous 0.05 mol dm $^{-3}$  acetic acid solution, HAuCl $_4$   $1 \times 10^{-3}$  mol dm $^{-3}$ , 0.2 mol dm $^{-3}$  isopropanol, pH 2.8, recorded 20 minutes after synthesis. Sonication time given in the figure.

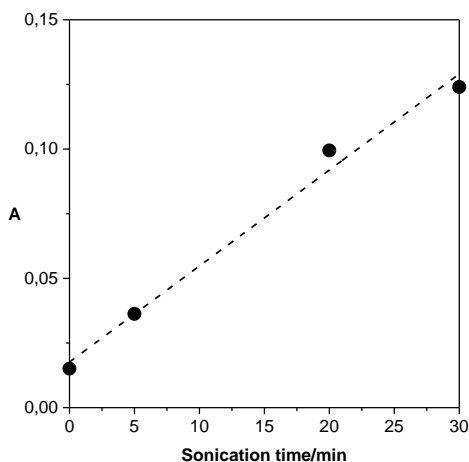


**Figure 3.** Sonolysis (620.2 kHz, nominal power 50 W, dose rate 74 W kg $^{-1}$ , 20 $^{\circ}$  C) of aqueous solution of  $1 \times 10^{-3}$  mol dm $^{-3}$  HAuCl $_4$ ,  $2 \times 10^{-3}$  mol dm $^{-3}$  chitosan and 0.2 mol dm $^{-3}$  isopropanol at pH 2.8 (CH $_3$ COOH). Increase in absorbance at  $\lambda = 537$  nm.



While sonolysis of water shows some resemblance to radiolysis, there are also marked differences between these two processes, which have been probably the cause of differences in the results of our two sets of experiments (see eqns. (1-7)). First of all, in sonochemistry the yield of oxidizing species ( $\cdot\text{OH}$ ) available for reaction with dissolved substrates is higher than the yield of reducing species ( $\text{H}^\cdot$ ). This is probably the reason why no net effect have been observed in isopropanol-free solutions. Secondly, efficiency of isopropanol in scavenging  $\cdot\text{OH}$  is expected to be much higher in sonolysis than in radiolysis. This effect stems from the fact that non-ionic compounds of partially hydrophilic and partially hydrophobic character (as aliphatic alcohols) have the tendency to accumulate at the surface of cavitation bubbles, i.e., in the zone where  $\cdot\text{OH}$  radicals escape from the gas phase of the bubbles out to the solution. Greatly enhanced local concentration of alcohol molecules in that zone makes them much more efficient  $\cdot\text{OH}$  scavengers (in comparison with ionic and thus strongly hydrophilic acetate and chitosan) than in radiolysis, where such local effects are absent. Therefore in sonochemical experiment nearly all  $\cdot\text{OH}$  radicals are efficiently converted into the reducing hydroxyalkyl radicals, which in turn can reduce chloroaurate ions. A side action of ultrasound is also the so-called mechanochemical effects, which by inducing high velocity gradients between adjacent layers of liquid are capable of breaking or fusion action on macromolecules and nanoparticles. From the location of the visible band and its red-shift in time we infer that in the studied case the fusion action was predominant, causing the initially formed AuNPs to coalesce. Position of the absorption maxima at wavelengths 533-556 nm suggest that AuNPs have larger dimensions than those synthesized by radiation. Okitsu et al. have shown that when Au nanoparticles are sonochemically formed (200 kHz, 200 W) in presence of chitosan powder, the maximum is located at 580 nm, which they claimed to correspond to the size of ca. 22 nm [20].

Data shown in Figs. 1 and 2 may be also a basis of preliminary quantitative estimates. Taking into account that  $3 e_{\text{aq}}^-$  or  $\text{H}^\cdot$  are necessary to reduce Au(III) in chloroaurate ions to Au(0),  $3 \times 10^{-3} \text{ mol dm}^{-3}$  of these species must be formed for the reaction to be complete. Since the combined yield of these species in radiolysis of water is ca.  $3.4 \times 10^{-7} \text{ mol J}^{-1}$ , a dose of 8.8 kGy should be sufficient for this purpose. This corroborates with the leveling off of the product absorbance with increasing dose in the 5-10 kGy range. In sonochemistry, assuming that all  $\text{H}^\cdot$  and  $\cdot\text{OH}$  (the latter via the hydroxyalkyl radicals) participate in reduction, and taking their total yield at 620.2 kHz as ca.  $3 \times 10^{-10} \text{ mol J}^{-1}$  [26], the required dose would be ca. 10 MGy. At the dose rate of  $74 \text{ Gy s}^{-1}$ , this dose would be reached after over 30 hours, thus the maximum sonication time of 30 minutes is clearly insufficient to make the reduction complete.

Similarly as for the radiation synthesis, chitosan seems to be a good stabilizing agent during and just after the sonochemical synthetic procedure, since no precipitation or pronounced aggregation of nanoparticles was observed. This is true despite the fact that both irradiation and sonication induce

degradation of chitosan, causing reduction of its average molecular weight [27-28]. The latter effect may be actually beneficial for the stabilizing effect. Shorter chains are more flexible, so they can easier interact with AuNPs and form the efficient protective layer at their surface.

### **3.2. Long-term stability of chitosan-gold nanoparticles**

One of the main factors of usability of metal nanoparticles is their stability in time. In order to evaluate the long-term stability of radiation- and sonochemically synthesized colloidal gold nanoparticles in the presence of chitosan as the stabilizing agent, absorption spectra have been recorded for up to 3 months after synthesis. These tests have been performed on the solutions irradiated with the dose of 2 kGy (i.e., when the reduction was not yet complete) in the absence and presence of 0.2 mol dm<sup>-3</sup> isopropanol (Fig. 4 a,b,c,d) and on solutions sonicated for 20 minutes in the presence of isopropanol (Fig. 5 a,b).

In all these cases the spectra undergo a slow time evolution. The intensity of plasmon resonance band increases without shift of its position, while in parallel a decrease in the substrate band at 212 nm is observed. The most important result, i.e., the stability of location of the band in the visible range, indicates that the AuNPs do not change their size over the tested period, so there is no apparent tendency towards aggregation. This is a clear indication that chitosan is a very good stabilizer of radiation- and ultrasound-synthesized gold nanoparticles.

Changes in the values of absorbance suggest that reduction process still takes place in tested systems during the storage period, although this process slows down with time. These data indicate that the average size of nanoparticles does not change, but their amount increases. It has been shown before that chitosan alone is capable of slow reduction of gold ions, and in our opinion this is the main reason of the observed changes. The reaction slows down when the substrate (chloroaurate) is depleted. One cannot exclude that other components of the system and/or their radiolysis/sonolysis products also contribute to the slow reduction process.

### **3.3. Hydrodynamic diameter and $\zeta$ potential of gold nanodispersion**

The size of the gold nanoparticles is an important aspect of their future applications in medical and industrial applications. When discussing the size of polymer-stabilized AuNPs, one should differentiate between the size of the gold nanoparticle itself (the core) and the size of the whole entity consisting of the core and polymer shell. Location of absorption band at the UV-Vis spectra yields approximate information on the core size, while the total size of the core-shell particle is of equal importance. The latter can be assessed by dynamic light scattering measurements of hydrodynamic radii. The data are shown in Table 1. Presented values indicate that AuNPs have hydrodynamic diameter ( $R_h$ ) in the range of several dozen nanometer in dependence on type and parameters of the synthesis.

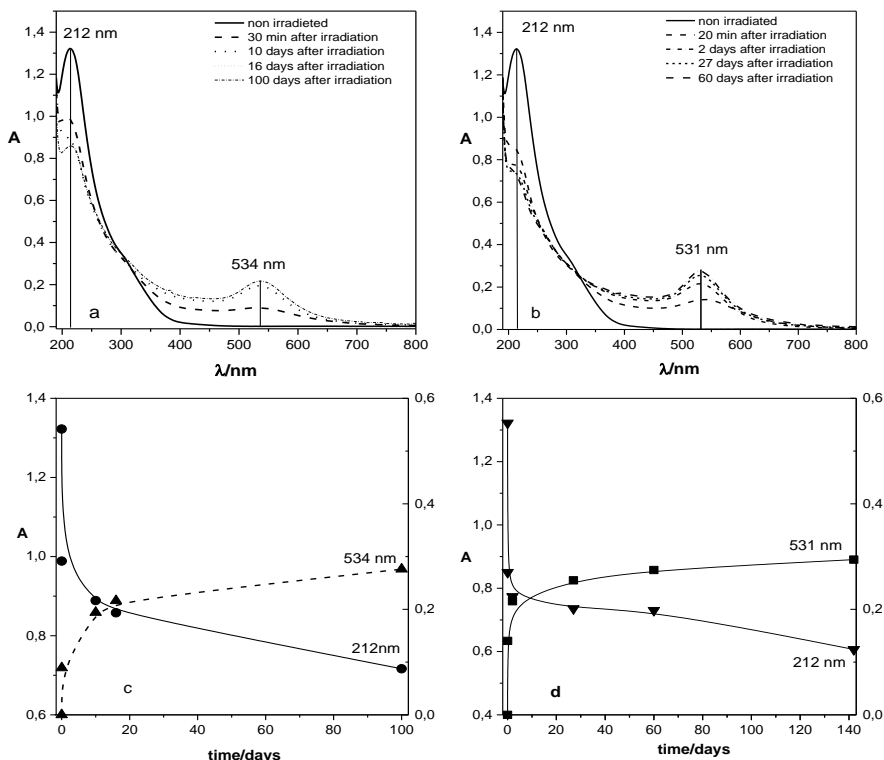


**Figure 4.** Absorption spectra of gold nanoparticles-chitosan dispersion before irradiation and after, a,c) without isopropanol, b,d) with  $0.2 \text{ mol dm}^{-3}$  isopropanol, irradiation dose was 2 kGy.

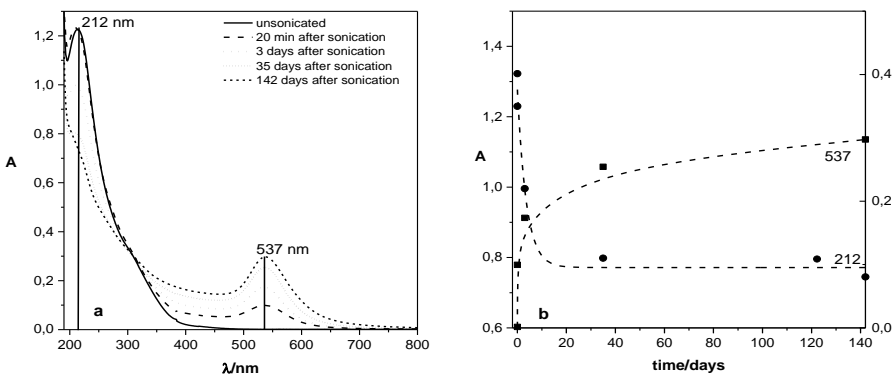


**Figure 5.** Changes in UV-Vis spectra of gold nanoparticles-chitosan dispersion obtained by sonication for 20 minutes.

Interestingly, the hydrodynamic radii mimic the tendencies of core size changes that can be followed by UV-Vis. Radiation synthesis at low doses results in relatively large  $R_h$  (29-37 nm), while by further irradiation these sizes are reduced down to 12-20 nm. This trend corresponds to the shift from ca. 530 to 510-518 nm in the location of the plasmon resonance band observed in Fig. 1. Presence of isopropanol seems to slightly reduce the core size (location of the absorbance band maxima at 518 nm without isopropanol and at 510 nm with isopropanol), while it apparently has a reverse effect on the shell size (20 nm vs. 12 nm, respectively) and on the polydispersity, which tends to be larger when isopropanol is present (PDI of ca. 0.23 vs 0.52, respectively). Exact nature of isopropanol influence is yet to be studied. Vo et al. after irradiation with doses of 5, 10 and 15 kGy obtained nanoparticles of average size 27, 12 and 7 nm (in terms of hydrodynamic diameter), respectively. These values are smaller than ours, for example for a dose of 10 kGy we obtained particles of 24 nm diameter. One of the sources of this difference can be different molecular weight of the applied chitosan (56 kDa in the work of Vo et al. vs. 158 kDa in our work).

Both UV-Vis and dynamic light scattering indicate that sonochemical synthesis, in the conditions applied here, leads to the formation of relatively large nanoparticles, of hydrodynamic radius higher than 30 nm. This roughly corresponds to the products of low-dose radiation synthesis, and in fact the location of their absorption maxima in UV-Vis are also similar. For nanoparticles obtained by sonication method, polydispersity index is relatively low, pointing to narrow size distribution of particles. Okitsu and co-workers reported influence of ultrasound frequency on average size of formed Au nanoparticles and rate of reduction Au(III). Using ultrasound at 647 kHz (nearly identical to 620.2 kHz used in our work) they obtained gold nanoparticles of 24 nm size [10].

For all synthesized gold nanoparticles, the values of zeta potential were higher than + 30 mV, which indicates that, due to the presence of positively charged chitosan chains at the surface of AuNPs, sufficiently high repulsive forces between the individual particles are present to prevent their aggregation. These results corroborate with the observed high long-term stability of nanoparticles, indicating that chitosan is indeed a good stabilizing agent for radiation- and ultrasound-synthesized nanoparticles.

**Table 1.** Hydrodynamic diameter (Z-average diameter), polydispersity index (PDI) and  $\zeta$  potential of gold nanoparticles synthesized by the radiation- and sonochemical methods. Measurements were carried out one hour after synthesis.

	Solutions	Dose [kGy]/ Sonication time [min]	$R_h$ [nm]	PDI	$\zeta$ potential [mV]
Irradiation	$1 \times 10^{-3}$ mol dm $^{-3}$ HAuCl $_4$ $2 \times 10^{-3}$ mol dm $^{-3}$ chitosan 0.2 mol dm $^{-3}$ isopropanol	1	29.2	0.57	48.0
		2	27.2	0.29	48.3
		5	36.8	0.52	33.9
		10	19.7	0.52	36.0
	$1 \times 10^{-3}$ mol dm $^{-3}$ HAuCl $_4$ $2 \times 10^{-3}$ mol dm $^{-3}$ chitosan	1	28.2	0.52	47.4
		2	16.3	0.36	47.1
		5	13.1	0.40	45.0
		10	12.2	0.23	36.7
Sonicati	$1 \times 10^{-3}$ mol dm $^{-3}$ HAuCl $_4$ $2 \times 10^{-3}$ mol dm $^{-3}$ chitosan 0.2 mol dm $^{-3}$ isopropanol	5	33.2	0.32	43.3
		20	45.8	0.25	45.0
		30	35.1	0.32	42.7

#### 4. Conclusions

Radiation and sonication methods can be applied, in appropriate conditions, to obtain particles of gold with nanometric size in aqueous solutions of chloroauric acid, when chitosan is used to stabilize the obtained particles. The particles exhibit characteristic absorption maxima in the UV-Vis absorption spectra, centered at 510-560 nm. Radiation synthesis initially leads to the formation of relatively large particles ( $R_h$  in the range of 29-37 nm), but at higher doses, corresponding to nearly complete substrate conversion, the average particle size goes down to ca. 12-20 nm, while sonochemical synthesis in the applied conditions leads to somewhat larger particles of  $R_h$  in the range of 33-45 nm. If synthesis conditions are chosen such that irradiation or sonication does not lead to complete conversion of chloroaurate ions to nanoparticles, a slow post-irradiation (post-sonication) reaction takes place, finally making the reaction complete. This effect is most probably due to a very slow spontaneous reduction of Au(III) to Au(0), mainly by chitosan, but maybe also by other components of the system. Due to the differences in mechanism of radiation- and ultrasound-induced reactions, presence of isopropanol doesn't seem to have a pronounced

effect on the radiation synthesis of AuNPs, while it is indispensable for efficient sonochemical synthesis.

Chitosan provides the gold nanoparticles with excellent stability, which is evidenced by high zeta potential (from +34 to +48 mV), lack of aggregation or precipitation and stability of localization of the UV-Vis plasmon resonance band for a period of at least 3 months. The exact mechanisms of interactions AuNPs with chitosan and stabilization process by chitosan definitely require further studies to be fully understood. The advantage of using radiation- or sonochemical synthesis, especially if AuNPs are intended for various biomedical and engineering applications, such as gold nanoparticles containing radioisotopes for targeted radiotherapy, is the lack of contamination by conventional reducing and capping agents, as well as simplicity of these methods and easy process control.

## **5. Acknowledgements**

*This work has been financed in part by the International Atomic Energy Agency (IAEA), Research Contract No: I 8354/R0, and National Science Centre, Poland (NCN), Contract No: UMO-2012/07/B/ST4/01429.*

## **6. Reference**

1. Louis C, Pluchery O; (2012) Gold nanoparticles for physics, chemistry and biology. *Imperial College Press*, London.
2. Christine-Daniel M, Astruc D; (2004) Gold nanoparticles: assembly, supramolecular chemistry, quantum-size-related properties, and applications toward biology, catalysis, and nanotechnology. *Chem Rev* 104, 293-346. DOI: 10.1021/cr030698+
3. Murugan M, Anthony K J P, Jeyaraj M, Rathinam N K R, Gurunathan S; (2014) Biofabrication of gold nanoparticles and its biocompatibility in human breast adenocarcinoma cells (MCF-7). *J Ind Eng Chem* 20, 1713-1719. DOI: 10.1016/j.jiec.2013.08.021
4. Schäffler M, Sousa F, Wenk A, Sitia L, Hirn S, Schleh C, Haberl N, Violatto M, Canovi M, Andreozzi P, Salmona M, Bigini P, Kreyling W G, Krol S; (2014) Blood protein coating of gold nanoparticles as potential tool for organ targeting. *Biomaterials* 35 (10), 3455-3466. DOI: 10.1016/j.biomaterials.2013.12.100
5. Cutler C S, Chanda N, Shukla R, Sisay N, Cantorias M, Zambre A, McLaughlin M, Kelsey J, Upenandran A, Robertson D, Deutscher S, Kannan R, Katti K; (2013) Nanoparticles and phage display selected peptides for imaging and therapy of cancer. *Recent Res Cancer Res* 194, 133-147.
6. Cutler C S, Hennkens H M, Sisay N, Huclier-Markai S, Jurisson S S; (2013) Radiometals for combined imaging and therapy. *Chem Rev* 113, 858-883. DOI: 10.1021/cr3003104

7. Doyen M, Bartik K, Bruylants G; (2013) UV-Vis and NMR study of the formation of gold nanoparticles by citrate reduction: Observation of gold-citrate aggregates. *J Colloid Interface Sci* 399, 1-5. **DOI:** 10.1016/j.jcis.2013.02.040
8. Gachard E, Remita H, Khatouri J, Keita B, Nadjo L, Belloni J; (1998) Radiation-induced and chemical formation of gold clusters. *New J Chem* 22, 1257-1265.
9. Caruso R A, Ashokkumar M, Grieser F; (2002) Sonochemical formation of gold sols. *Langmuir* 18, 7831-7836. **DOI:** 10.1021/la020276f
10. Okitsu K, Ashokkumar M, Grieser F; (2005) Sonochemical synthesis of gold nanoparticles: effects of ultrasound frequency. *J Phys Chem B* 109, 20673-20675. **DOI:** 10.1021/jp0549374
11. Sakai T, Enomoto H, Sakai H, Abe M; (2014) Hydrogen-assisted fabrication of spherical gold nanoparticles through sonochemical reduction of tetrachloride gold(III) ions in water. *Ultrason Sonochem* 21, 946-950. **DOI:** 10.1016/j.ultsonch.2013.12.010
12. Spothem-Maurizot M, Mostafavi M, Douki T, Rigny P; (2008) Radiation chemistry. From basics to applications in material and life sciences. EDP Sciences, Les Ulis.
13. Dash M, Chiellini F, Ottenbrite R M, Chiellini E; (2011) Chitosan - a versatile semi-synthetic polymer in biomedical applications. *Prog Polym Sci* 36, 981-1014. **DOI:** 10.1016/j.progpolymsci.2011.02.001
14. Croiser F, Jerome C; (2013) Chitosan-based biomaterials for tissue engineering. *Eur Polym J* 49, 780-792. **DOI:** 10.1016/j.eurpolymj.2012.12.009
15. Hu L, Mao Z, Gao C; (2009) Colloidal particles for cellular uptake and delivery. *J Mater Chem* 19, 3108-3115. **DOI:** 10.1039/B815958K
16. Wei D, Qian W; (2008) Facile synthesis of Ag and Au nanoparticles utilizing chitosan as a mediator agent. *Colloids Surf B* 62, 136-142. **DOI:** 10.1016/j.colsurfb.2007.09.030
17. Cazacu A, Bindar D, Tartau L, Hritcu L, Stefan M, Nita L, Ionescu C, Nica V, Rusu G, Dobromir M, Melnig V; (2011) Effect on nerve structures of functionalized gold-chitosan nanoparticles obtained by one pot synthesis. *Ann Univ Iasi* 12, 45-51.
18. Vo K D N, Guillon E, Dupont L, Kowandy C, Coqueret X; (2014) Influence of Au(III) interaction with chitosan on gold nanoparticles formation. *J Phys Chem C* 118, 4465-4474. **DOI:** 10.1021/jp4112316
19. Vo K D N, Kowandy C, Dupont L, Coqueret X, Hien N Q; (2014) Radiation synthesis of chitosan stabilized gold nanoparticles comparison between  $e^-$  beam and  $\gamma$  irradiation. *Radiat Phys Chem* 94, 84-87. **DOI:** 10.1016/j.radphyschem.2013.04.015
20. Okitsu K, Mizukoshi Y, Yamamoto T A, Maeda Y, Nagata Y; (2007) Sonochemical synthesis of gold nanoparticle on chitosan. *Mat Lett* 61, 3429-3431. **DOI:** 10.1016/j.matlet.2006.11.090

21. Rosiak J M, Ulanski P, Al-Assaf S; (2009) Protocol for determination of intrinsic viscosity of chitosan, IAEA Co-ordinated Research Programme: Development of Radiation-Processed Products of Natural Polymers for Application in Agriculture, Healthcare, Industry and Environment; International Atomic Energy Agency: Research Coordination Meeting, Reims, France, 201-221.
22. ISO/ASTM51607-13. Standard Practice for Use of the Alanine-EPR Dosimetry System.
23. Oh E, Susumu K, Goswami R, Mattoussi H; (2006) One-phase synthesis of water-soluble gold nanoparticles with control over size and surface functionalities. *Langmuir* 26, 7604–7613. **DOI:** 10.1021/la904438s
24. Ulanski P, von Sonntag C; (2000) OH-radical-induced chain scission of chitosan in the absence and presence of dioxygen. *J Chem Soc Perkin Trans 2* 10, 2022-2028.
25. Li T, Park H G, Choi S H; (2007)  $\gamma$ -Irradiation-induced preparation of Ag and Au nanoparticles and their characterizations. *Mat Chem Phys* 105, 325-330. **DOI:** 10.1016/j.matchemphys.2007.04.069
26. von Sonntag C, Mark G, Tauber A, Schuchmann H P; (1999) OH radical formation and dosimetry in the sonolysis of aqueous solutions. *Adv Sonochem* 5, 109-145.
27. Czechowska-Biskup R, Rokita B, Lotfy S, Ulanski P, Rosiak J M; (2005) Degradation of chitosan and starch by 360-kHz ultrasound. *Carbohydr Polym* 60, 175-184. **DOI:** 10.1016/j.carbpol.2004.12.001
28. Czechowska-Biskup R, Rokita B, Ulanski P, Rosiak J M; (2005) Radiation-induced and sonochemical degradation of chitosan as a way to increase its fat-binding capacity. *Nucl Instr Meth Phys Res B* 236, 383-390. **DOI:** 10.1016/j.nimb.2005.04.002